

III/V Device Optimization by Physics-Based S-Parameter Simulation

R. Quay¹, V. Palankovski², R. Reuter¹, M. Schlechtweg¹,
W. Kellner³, S. Selberherr²

¹ Institute of Applied Solid-State Physics, Tullastr. 72, D-79108 Freiburg, Germany.

² Institute for Microelectronics, TU Vienna, Gusshaustr. 27-29, A-1040 Vienna, Austria.

³ Infineon Technologies AG, Corporate Research, Otto Hahn Ring 6, D-81730 Munich, Germany.

Abstract We demonstrate two-dimensional simulations for design of AlGaAs/InGaAs/GaAs High Electron Mobility Transistors (HEMTs) with gate-lengths ≤ 150 nm with emphasis on power applications in the Ka-band and of AlGaAs/GaAs Heterojunction Bipolar Transistors (HBTs). Besides the use of advanced interface and generation/recombination models the simulations yield the bias dependence of the small signal equivalent circuit elements.

1. Introduction

GaAs based HEMTs and HBTs are finding increasing application. In the course of this process the development of Technology Computer Aided Design (TCAD) tools such as the device simulator MINIMOS-NT is subject to continuous efforts to satisfy the ongoing demand for optimization. The performance with respect to DC and RF capabilities has been demonstrated for several material systems and devices [1-2]. Power applications in the Ka-band are promising markets for HEMTs. Simulation tools to predict DC, RF, and thermal properties are necessary to meet challenging power requirements in the material system. Further understanding of the bias dependence of the RF small signal equivalent elements, especially on the drain-source voltage V_{DS} , is necessary to optimize devices in this frequency range. Since the bias dependence is caused by various parameters interacting on device performance, the simulations are used for the design of experiments [3] to reduce the costs of development. At the same time the AlGaAs/GaAs HBTs enter the market for cellular phone applications. It is therefore very desirable to describe the RF characteristics on a physical base as shown in this work.

2. Simulation

The HEMT simulations shown in this work include hydrodynamic simulation in combination with a thermionic field emission interface model in HEMTs with gate-lengths of $l_g=120$ nm to 150 nm. The results obtained for HEMTs are based on two different technologies, further named I and II. HEMTs and HBTs are simulated using the same set of simulation parameters.

The S-parameters are simulated with MINIMOS-NT at a frequency of 5 GHz and calculated up to 120 GHz for the HEMT using the standard eight element small signal equivalent circuit. The connection of the device simulator and the parasitic circuit environment was improved to obtain better agreement of measured and physically simulated S-parameters. The understanding of the simulation of contact properties is vital when comparing the two

HEMT technologies with different cap geometries. For the HBT simulations band gap narrowing, surface recombination, and minority carrier mobility are considered in the simulations [6]. The RF extraction is performed similarly to the HEMT. The f_T and f_{max} values are extracted from the calculated element lh_{21} and from the maximum available gain MAG, respectively.

3. RF Results

Fig. 1 shows the measured and simulated output characteristics of a GaAs PHEMT with a gate-length $l_g=150$ nm of technology I. Note the agreement of the simulation in comparison to the measurement. Results of the same precision were obtained with exactly the same simulation parameters as used for HEMT technology II. The only fundamental difference in the simulation is the modeling of the source and drain ohmic contacts. Due to different cap geometries and contact processing performed technology I can best be described using direct contacting of the AlGaAs spacer to the ohmic contact whereas technology II can best be described by assuming the ohmic contacts on top of the caps.

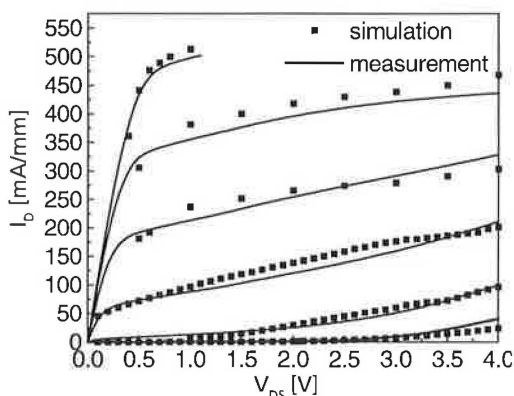


Fig. 1 Output-characteristics of a GaAs PHEMT, technology I, dots: simulated, lines: measurement V_{GS} in 0.2 V steps from $V_{GS}=-0.8$ V.. 0.2 V.

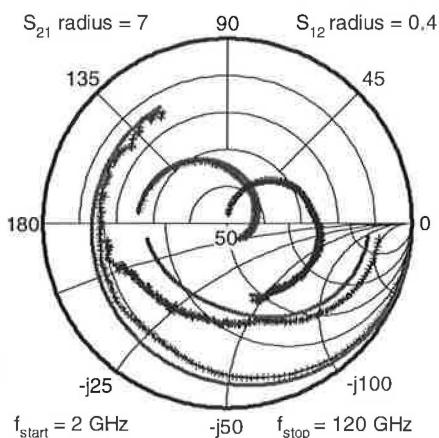


Fig. 2 Simulated (lines) and measured (+) S-parameters of a HEMT, technology II, $V_{DS}=2.0$ V, $V_{GS}=0.4$ V.

The accurate DC simulations are a prerequisite for a physically-based prediction of the S-parameters of the device [4]. Fig. 2 shows a comparison of measured and simulated S-parameters at a typical class A bias condition for a HEMT of technology II with a gate-length $l_g=120$ nm. Due to improvements in the hydrodynamic interface models, a good agreement of measured and simulated S-parameters in the frequency range from 2 to 120 GHz is achieved suitable for prediction of circuit design. Further it is found that the proper DC simulation of the gate current is a key to extract most accurate RF elements from the physical simulation.

For better large signal/power performance a workable goal of device optimization is the reduction of the bias dependence of the current gain cut-off frequency f_T with increasing drain-source voltage V_{DS} or collector current I_C for the HEMT and HBT, respectively. For HEMTs this includes the necessity of understanding the physical origins of the bias dependence of g_m , C_{gs} , and C_{gd} varying V_{DS} and the gate-source voltage V_{GS} . By variations of doping, of the description of contact alloying in the caps and of the geometry (see [4-5]), the dependence of V_{DS} is investigated for various structures for the HEMT. Fig. 3 shows the bias

dependence of the gate-drain capacitance C_{gd} as a function of V_{DS} at constant V_{GS} of a HEMT of $l_g = 150$ nm for various cap doping concentrations over a wide parameter range. C_{gd} is a decreasing function of V_{DS} due to the increase in size of the depletion zone in the cap at the drain end of the gate, as can be directly seen from the simulation results. The change in the conduction properties by the doping variations alters the currents drastically and determines the magnitude of C_{gd} at a given V_{DS} .

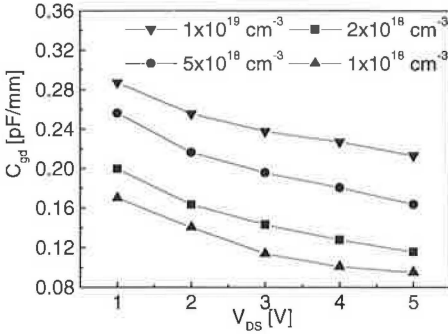


Fig. 3 Simulated dependence of C_{gd} on V_{DS} , parameter: cap doping concentration.

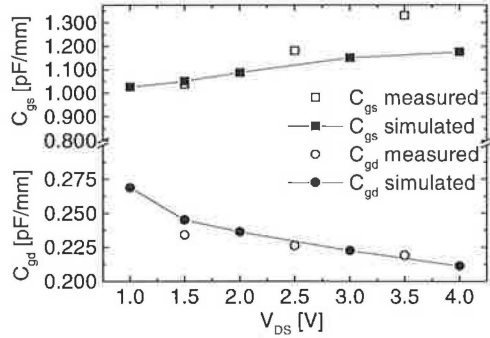


Fig.4 Dependence of C_{gs} and C_{gd} as a function of V_{DS} and comparison to measurements.

For C_{gs} it is found that the dependence on V_{DS} is influenced by a variety of parameters, where the origins of the major contributions to the dependence of C_{gs} on V_{DS} are strongly correlated to the device structure. Fig. 4 shows the simulated and measured dependence of C_{gs} and C_{gd} as a function of V_{DS} at constant V_{GS} . C_{gs} increases with V_{DS} . For achieving a relatively small increase of C_{gs} with V_{DS} , the carrier density in the channel caused by the delta doping and the cap doping concentrations has to be optimized with respect to the ohmic contacting of the channel, since the contacting strongly influences the distribution of the electric field in the channel.

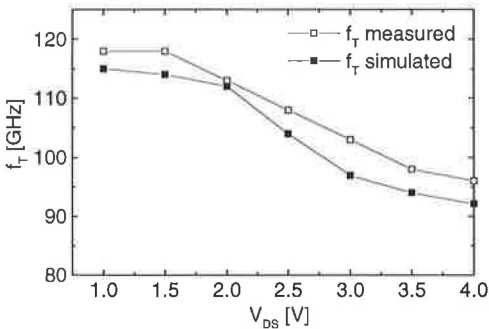


Fig. 5 Simulated and measured decrease of f_T for a HEMT of 140 nm gate-length.

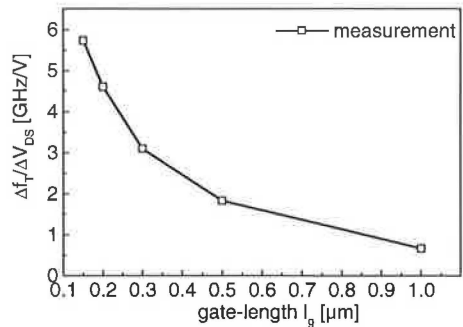


Fig. 6 Measured decrease of $\Delta f_T / \Delta V_{DS}$ as a function of gate-length l_g .

As can be seen in Fig. 5, the transit frequency f_T is a decreasing function with V_{DS} and constant V_{GS} for the investigated HEMT with gate-length $l_g = 140$ nm. It is found that the

decrease in f_T with V_{DS} is a strong function of the gate-length as is shown by measurements on processed devices in Fig. 6. It shows the extracted decrease $\Delta f_T/\Delta V_{DS}$ from measured S-parameters as a function of gate-length for one type of pseudomorphic depletion HEMT. This graph is an example that short channel effects are very relevant for the large signal device performance.

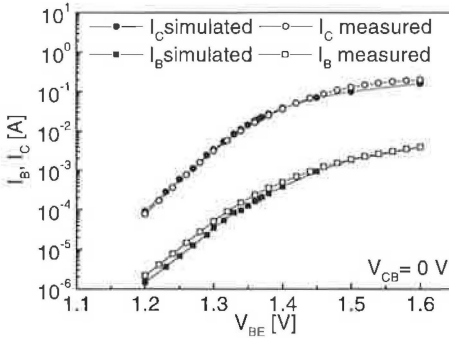


Fig. 7 Simulated and measured forward Gummel plot of an AlGaAs/GaAs HBT at $T=296$ K.

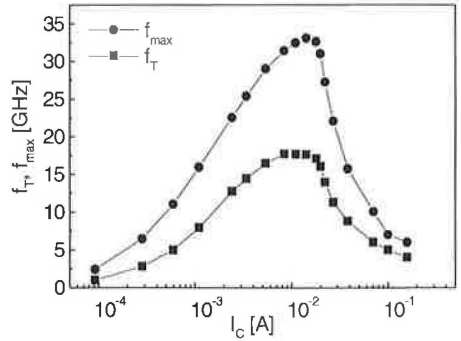


Fig. 8 Simulated f_T/f_{\max} vs. I_C for an HBT at $V_{CB} = 0$ V, $T=296$ K.

In Fig. 7 a comparison of the simulated and measured forward Gummel plots of a single finger AlGaAs/GaAs HBT with an emitter area of $90 \mu\text{m}^2$ is shown. On the base of these precise DC results Fig. 8 shows the simulated dependence of f_T and f_{\max} on the collector current I_C analogous to the Gummel plot at $V_{CB} = 0$ V and increasing V_{BE} for the same structure. From that a maximum $f_T = 17.6$ GHz and a $f_{\max} = 33$ GHz are extracted.

4. Conclusion

We have demonstrated the use of two-dimensional simulations for the determination of RF small signal characteristics for HEMT and HBT. Thus, III/V device simulation can actively support industrial development of relevant device structures.

5. Acknowledgments

The authors would like to acknowledge the support of Siemens AG and the German ministry of education and research (BMBF).

6. References

- [1] Brech H Grave T Simmlinger T Selberherr S 1997 *IEEE Trans. Electron Devices* **44** 1822-1828
- [2] Grasser T Palankovski V Schrom G Selberherr S 1998 in: de Meyer K K Biesemans S (eds.) *Simulation of Semiconductor Processes and Devices* 247-250 (Wien, Springer)
- [3] Atherton J S Snowden C M Pollard R D 1995 *Proc. European Microwave Conference* Bologna 1017-1019
- [4] Quay R Reuter R Palankovski V Selberherr S 1998 *Proc. IEEE Workshop Electron Devices Microwave Optoelectronic Applications* Manchester 13-18
- [5] Wu C S Pao C K Yau W Kanber H Hu M Bar S X Kurdoghlian A Bardai Z Bosch D Seashore C Gawronski M 1995 *IEEE Trans. Microwave Theory Techniques* **43** 257-263
- [6] Palankovski V Selberherr S Schultheiss R 1999 *Proc. Simulation of Semiconductor Processes and Devices* Kyoto